30th Symposium on Naval Hydrodynamics
Hobart, Tasmania, Australia, 2-7 November 2014

Split-Time Method for Pure Loss of Stability and Broaching-To

K. J. Spyrou[1], V. Belenky[2], A. M. Reed[2], K. Weems[3], N. Themelis[1], I. Kontolefas[1]
([1]National Technical University of Athens, Greece; [2]David Taylor Model Basin / NSWCCD, Maryland, USA; [3]Leidos, Inc., Maryland, USA)

ABSTRACT

Dynamical aspects related to the application of the split-time method for the probabilistic assessment of ship dynamic stability failure caused by pure loss of stability and broaching-to are considered. Changes of stability in waves can cause a large roll angle by the timing of those changes, even if the duration of the stability degradation is not very long. An idea for a metric of the likelihood of stability failure is introduced. For pure loss of stability, the difference between the critical and instantaneous roll rates at the instant of upcrossing of an intermediate level has been found to be an effective metric. This metric can be related to Euler's definition of ship stability and, in general, to the definition of stability in mechanics.

The consideration of broaching-to focuses on surf-riding in irregular waves. A new method is considered for the calculation of the wave celerity in irregular waves, based on the concept of instantaneous frequency. The new scheme provides a smoother time history in comparison to a previous scheme that was based on the propagation speed of characteristic features of the wave profile. Irregular waves render the phase flow associated with ship surging and surf-riding time-dependent. The method of "Feature Flow Field" is introduced for effectively analyzing it. The candidate for a metric of the likelihood of surf-riding is the straight line distance, in the phase plane, between the state of a ship and the stable surf-riding equilibrium at that instant.

INTRODUCTION

This paper examines two modes/scenarios of dynamic stability failures: pure loss of stability and broaching-to preceded by surf-riding. Pure loss of stability is a result of the deterioration of stability when a ship is positioned on a wave crest. Surf-riding is a phenomenon of the ship's acceleration to wave celerity when a wave "captures" the ship on its front slope. At times, a ship may not be directionally stable while surf-riding, and the ship could experience broaching-to—a phenomenon of a violent turn despite maximum steering effort—that may induce a large roll angle or even capsizing.

Dynamic stability failures in following and quartering seas may occur through a variety of scenarios. All of them are considered to be complex and difficult to analyze, even in regular waves. For example, broaching-to in regular, stern quartering waves requires the study of dynamics in multi-dimensional phase-space (Spyrou, 1996). A mathematical model of four ordinary differential equations (ODE), which can be considered as the minimum for capturing the essential phenomena, provides very rich dynamics because a number of bifurcations can arise in such a dynamical system.

However, mathematical models based on ODEs serve only as a rough approximation of ship dynamics. Advanced numerical codes (Beck and Reed 2001) potentially provide a more realistic description of ship motion, though at the expense of introducing further complexity to an already complex dynamical system. Key features of the advanced models are the inseparability of excitation and stiffness and the hydrodynamic memory effect. Nonetheless, one can still apply the analysis tools of nonlinear dynamics and the result has been shown to be qualitatively very similar to the ODE solution (Spyrou *et al.* 2009). The hydrodynamic memory effect may be treated in ODEs by including additional degrees of freedom (Spyrou and Tigkas 2011).

Accounting for irregular waves in the mathematical model of broaching-to generates a whole new series of issues. To begin with, the problem must be considered simultaneously in time and in space, whereas spatial consideration is sufficient in regular waves. The state of surf-riding becomes a "quasi-equilibrium" as it appears and disappears randomly (Belenky, *et al.,* 2013). Moreover, wave celerity in irregular waves becomes random and the evaluation of a condition of capture based on it becomes an intriguing problem (Spyrou, *et al.,* 2014).

The complexities of modeling for pure loss of stability are also related with the randomness of irregular waves. The calculation of stability changes in regular waves does not pose a technical problem and has been included in many hydrostatic software packages, and the calculation of the time-varying roll restoring (GZ)

curve in irregular wave simulations has been demonstrated (Belenky, *et al.*, 2010). However, the development of an ODE-like model of the stability changes has not proved to be viable (see the next section), so hydrodynamic analysis cannot be effectively performed with a purely ODE-based model.

The split-time method may be seen as a way of handling complex dynamical systems when the probability of a specific rare event must be found. While the method has evolved significantly over the course of its development (Belenky, *et al.*, 2008, 2010, 2013), the principal idea remains unchanged. This idea is to separate a complex problem in two, less complex elements. The first problem is to estimate an upcrossing through an intermediate level ("non-rare" problem), while the second is to determine the probability of a rare event (capsize or attraction of surf-riding equilibrium) once the upcrossing occurs ("rare" problem).

Figure 1 shows the basic scheme for applying the split-time method for capsizing. While the figure looks exactly the same as in Belenky, *et al.* (2013), the numerical scheme has been changed. The "non-rare" problem has become purely statistical; simulations are run until sufficient statistics of upcrossing have been collected (consideration of how to set this intermediate level will be found in the second section of this paper). The "rare" problem consists of a series of short simulations to find conditions leading to the event of interest at the instant of upcrossing. In case of capsize, the minimal initial conditions consist of roll angle and roll rate. Since the roll angle is defined by the intermediate level, the roll rate leading to capsizing is the only unknown to be found.

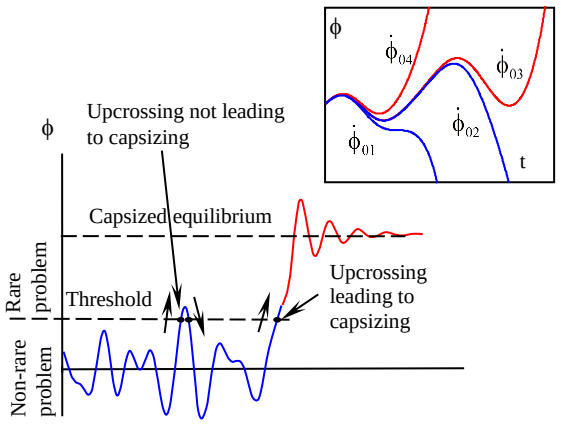

Figure 1: General Scheme of Split-time Method for Capsizing

The roll rate leading to capsizing at the instant of upcrossing is identified as the "critical" roll rate, and is calculated for each upcrossing. The difference between the observed and critical roll rate at the instant of upcrossing is the metric of danger; once this difference is zero, capsizing becomes inevitable.

The primary focus of this paper is to study the dynamical properties of roll-rate difference as a "metric for likelihood of capsizing." We then attempt to formulate a corresponding metric for the problem of surf-riding. The statistical properties of the metric are outside the scope of this paper, and are presented in Belenky, *et al.* (2014).

PURE LOSS OF STABILITY

Dynamical Mechanism of Pure Loss of Stability

The difference between ship stability in waves as compared to calm water has been known in Naval Architecture for well over a century (Pollard & Dudebout, 1892). However, practical calculation methods were not available until the 1960s (Paulling, 1961). A decade later, it was recognized as a separate mode of stability failure (Paulling, *et al.*, 1975).

The classic scenario of pure loss of stability involves a prolonged exposure to reduced stability on a wave crest, which results in a large roll angle or even capsize. An obvious approach to examining this phenomenon was to consider the elements of stability as random quantities (Dunwoody, 1989a), which leads to the probability of a certain ship response (Dunwoody, 1989b). The development of advanced hydrodynamic codes have revealed a more complex picture of the phenomenon.

The following results illustrate the mechanics of a large roll event in irregular seas. The ship is the ONR Topside Series tumblehome configuration (Bishop, *et al.*, 2005) and the condition is Sea State 8 (significant wave height 11.5 m, modal period 16.4 s) at zero speed in stern quartering long-crested seas. Time-domain simulations are made using the Large Amplitude Motion Program (LAMP; *cf.* Lin & Yue, 1990). The simulations use the LAMP-2 solver (nonlinear body-wave formulation for Hydrostatic and Froude-Krylov forces, with radiation and diffraction forces evaluated over the mean wetted surface), three degrees-of-freedom were allowed (heave, roll, pitch). The simulations were performed for several random realizations of the seaway and the instantaneous GZ curve is computed at each time step of the simulations (Belenky, *et al.*, 2010).

A very large roll angle of 47.94 deg was recorded around 281 s of one of the simulations. Figures 2–5 present instantaneous GZ curves for the half of a response period containing the large roll angle. Each of the figures is supplemented with a roll time history, containing this large roll angle. The instantaneous ship position is marked with a square on the GZ curve figure and with a vertical line on the time history plot.

The situation shown in Fig. 2 is fairly normal. The ship has a moderately large roll to starboard (positive roll angle in this system) and the GZ curve, which is the stiffness of the dynamical system, goes through zero with positive slope, indicating the presence of a stable equilibrium near the upright position.

Figure 3 shows the instant when the roll angle reaches zero value. The topology of the GZ curve is no longer normal; stable equilibrium around zero roll angle is absent. There is no stability on the port side; the stiffness is positive for negative roll angle. It means the restoring moment will act opposite to normal: instead of resisting further heeling, it pushes the ship over.

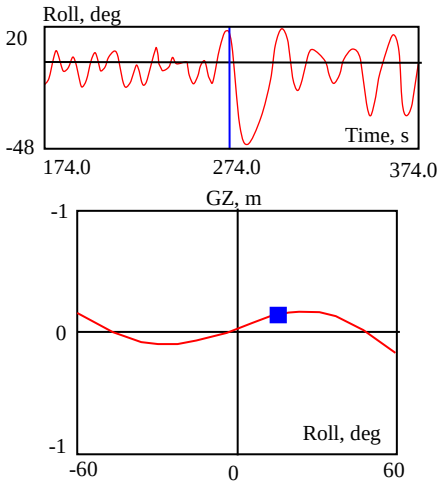

Figure 2: Roll **Time** History (above) and Instantaneous GZ Curve (below); Initial Stage

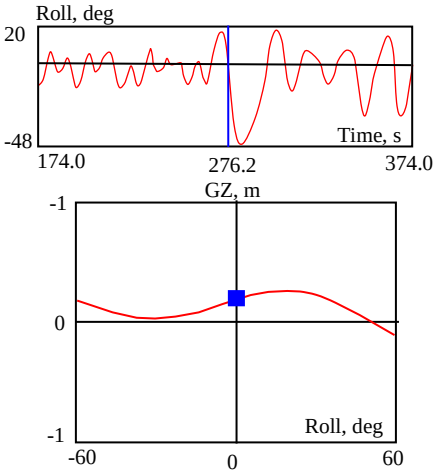

Figure 3: Roll Time History (above) and Instantaneous GZ Curve (below); Zero Roll Angle

In Fig. 4, the roll angle increases rapidly, but after about 1.4 s, the near-zero equilibrium appears again. The stability to port has been partially regained, while the stability to starboard has disappeared completely. The ship is practically at equilibrium but this equilibrium is unstable. The instantaneous GZ curve almost touches the axes near the zero on the positive side; it may be "the residue" from the positive peak of the GZ curve that was observed in Fig. 3. There is still no stability further to port (to the left of the square showing instantaneous ship position on the GZ curve).

Judging by the GZ curve shown in Fig. 4, the situation seems to be heading towards capsize. As indicated in the time history, however, capsize does not occur and Fig. 5 shows why. After about 5 s, stability to port has been restored; this resists further heeling and finally stops the roll at 47.94 degrees. There is still no stability for roll to starboard, but it does not matter at this point as the ship is heeled to port.

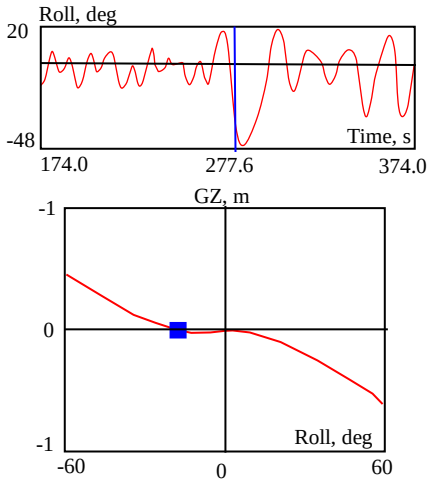

Figure 4: Roll Time History (above) and Instantaneous GZ Curve (below); **Zero** Stiffness

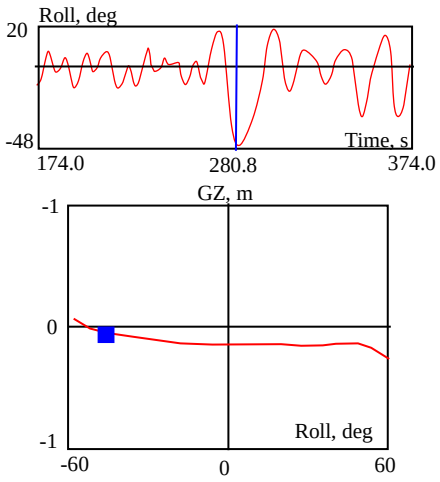

Figure 5: Roll Time History (above) and Instantaneous GZ Curve (below); Amplitude Roll Angle

The duration of negative stability to port was about 3.6 s (from 274 s in Fig. 2 until 277.6 s in Fig. 4), and this exposure was sufficient to cause a very large roll angle. The persistence of exposure to reduced or negative stability seems to be insufficient to completely allow the phenomenon of pure loss of stability to occur; the timing or phase of the stability reduction is also very important.

The drastic changes in the GZ curve topology leave very little chance of effectively modeling it by "modulating" the calm-water GZ curve with random GM value. The characterization of the equilibria is at least as important as the randomness of the GM value.

Of course, the mechanism of the described event is not the only one that may produce a larger roll, but it is

clear that pure loss of stability is a complex dynamical phenomenon.

Stability of a Ship and Stability of Motions

The computation of the instantaneous GZ curve, as described in the previous subsection, has left very little hope of developing a simple model of GZ curve changes in waves. The direct computation of the GZ in waves is possible, but is computationally expensive to perform at every step of long simulations. This led to the idea of searching for capsizing conditions (critical roll rates) only at the instants of upcrossing of some intermediate level of roll angle.

The algorithm of this search is illustrated in Fig. 6. The roll rate at the upcrossing is perturbed by a small amount, and a new simulation is run from the point of upcrossing. The initial roll angle equals the intermediate (threshold) level, while the initial roll rate equals the perturbed roll rate. Heave and pitch are currently taken from the unperturbed simulation, but full free motion could be considered in the future.

The value of the roll rate perturbation is increased until the simulation shows capsizing. Then the critical roll rate can be computed (with a given tolerance) by iteration, handling the problem in a manner similar to the numerical solution of a set of algebraic equations.

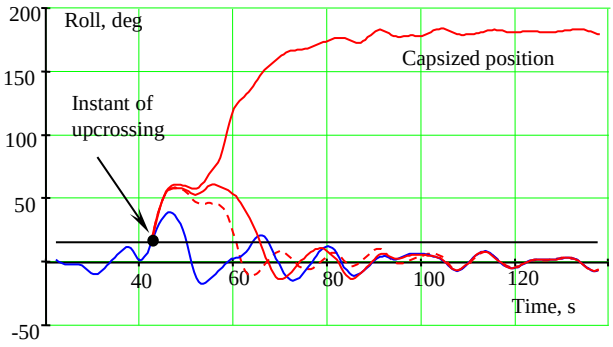

Figure 6: Calculation of the Critical Roll Rate

This algorithm may be interpreted as a definition of stability. Euler (1749) defined a stable ship as "being inclined by external forces returning back to its original position, once the forces ceased to exist". The perturbation of the roll rate can be considered as a dynamic application of a force. Indeed, if a force is applied for a short time, the result of such application is change in momentum, *i.e.* change in roll rate. Thus, this roll rate perturbation is the "Euler's force" that was applied and then "ceased to exist" in order to determine ship's stability. The critical roll rate can therefore be considered as a metric of the stability range from the point of view of this classical definition of ship stability.

As shown in Fig. 6, the perturbed time history converges with the unperturbed motions if capsize does not occur,. This allows the capsizing definition to be interpreted from the standpoint of general motion stability. The response of a dynamical system is defined as (asymptotically) stable if, after a perturbation, the perturbed response tends to the unperturbed response. Thus, capsizing, as determined by a critical roll rate, may be seen as "an instability" in roll motion. Then, the critical roll rate is used as a metric of motion stability, as it includes the magnitude of perturbation leading to "an instability" at a particular instant of time.

This discussion has established equivalency between the proposed algorithm for critical roll rate and accepted definitions of stability of a ship and general motions stability. Moreover, one can demonstrate that the classical definition of ship stability in calm water is equivalent to general motion stability definition through the critical roll. This method of solution of "rare problem"—by searching a critical value for perturbation—is subsequently referred to as the Motion Perturbation Method, or MPM.

The Intermediate Level

One important question remains: what is the intermediate level and how can it be determined? The meaning of the intermediate level has changed with the evolution of the split-time method. The initial version of the method (Belenky, *et al.*, 2008, 2010, 2013) interpreted the intermediate level as the boundary between two different domains with different physics, such as attractor and repeller, increasing and decreasing parts of the GZ curve. That led to requiring a very specific location for the intermediate level. As a result, there was a need to track the GZ curve in waves and to theoretically evaluate the upcrossing rate, as there was no guarantee that enough statistical data would be available.

The MPM-based approach does not have any particular requirement for the location of the intermediate level from the physical standpoint. The role of the intermediate level is different here; it provides the relationship between probability and time. Many authors have used Poisson flow as a model for capsizing in irregular seas, so the probability of capsizing after time T is:

$$P(T) = 1 - \exp(-\lambda T) \qquad (1)$$

Here λ is a rate of capsizing. Following the logic of Belenky, *et al.* (2008), capsizing occurs at an upcrossing, where the observed roll rate at upcrossing exceeds the critical roll rate:

$$\lambda = \lambda_U \cdot \int_{\dot{\phi}_{cr}}^{\infty} pdf(\dot{\phi}_U)\, d\dot{\phi}_U \qquad (2)$$

Where $\dot{\phi}_U$ is the roll rate at the instant of upcrossing, $\dot{\phi}_{cr}$ is the critical roll rate found with MPM, *pdf* stands for probability density function, and λ_U is the rate of the upcrossing of the intermediate level.

As noted above, the intermediate level is now chosen in such a way that a statistically significant number of upcrossing events can be observed. The value of the upcrossing rate can therefore be estimated directly from observations:

$$\hat{\lambda} = \frac{N_U}{T} \tag{3}$$

Where $\hat{\lambda}$ is an estimate of the upcrossing rate through the intermediate level, N_U is the number of observed upcrossings, and T is the total time of observation but *not* the same T as in (1).

If the intermediate level is chosen high enough that the upcrossings can be considered independent, the confidence interval of the estimate (3) can be evaluated using the normal distribution (Belenky, *et al.*, 2008). However, the current (MPM) version of the split time method does not require Poisson flow for the intermediate level. Yet there are other considerations.

To avoid additional complexities, it is better to keep random values of critical roll rate independent. The situation shown in Fig. 7a suggests that the two values of critical roll rate will be independent, because the second upcrossing occurred after the perturbed solution has converged to the unperturbed solution. Thus, whatever happens at the first upcrossing has no influence on the next upcrossing.

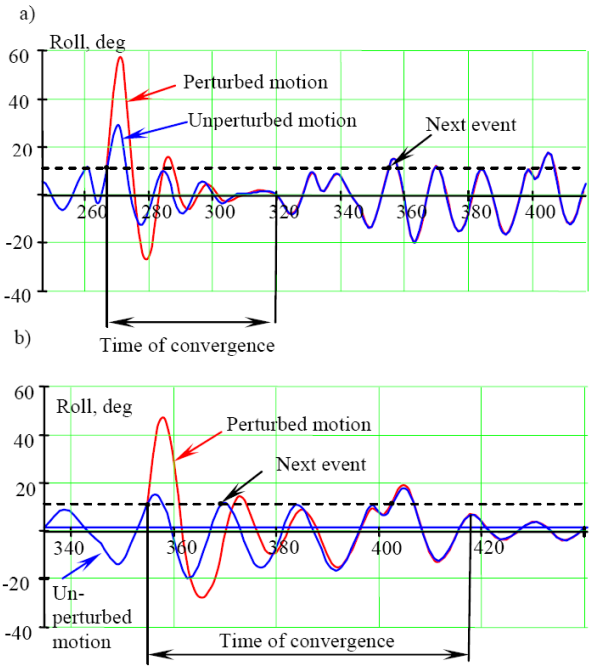

Figure 7: Independent (a) and Dependent (b) Upcrossing Events from the Point of View of the Critical Roll Rate

The situation shown in Fig. 7b is different. The second upcrossing is located within the time of convergence. As a result, the critical roll rates evaluated for these two upcrossing events may be dependent. This is important, as the construction of *pdf* in (2) will require independent data (Belenky, *et al.*, 2014).

The appearance of dependent upcrossings does not disqualify the selected intermediate level. It is simply necessary to use only one of each set of dependent upcrossing events for calculations requiring independent data. Note that the check of the independence of the results of sequential critical roll rate calculations imposes no additional burden, as the convergence time is available from the MPM analysis.

However, if the intermediate level is too low, there will be many dependent critical roll rate calculations and many of the data points will be disqualified; this means that some computations will be wasted. On the other hand, if the intermediate level is too high, there will be very few upcrossing observations, and one will need to run the code for a long time to collect a sample of sufficient size.

SURF-RIDING

Celerity of Irregular Waves

In regular (periodic) waves, surf-riding occurs when a ship's instantaneous surge velocity reaches wave celerity. One wonders, however, whether this simple phenomenological condition could be extended to an irregular wave environment. An issue that arises is how wave celerity should be calculated for a polychromatic sea. Recently, the concept of *instantaneous celerity* was introduced, built upon the velocity of the propagation of a suitable local property of the wave profile (Spyrou, *et al.*, 2012, 2014). In parallel, a variant definition (but still under the same principle) referring to *local celerity* was proposed, based on the propagation in time-space of the point of maximum wave slope located in the vicinity of the ship, as an approximate and observable representative of the position of maximum surge wave force nearest to the ship. These celerity functions can sometimes show an intensely fluctuating character and may jump to infinity (the result for example of a process of generation and annihilation of wave crests) especially for broader spectral bandwidths. Such a feature is undesirable as it must be continually checked against the ship surge velocity. We have thus introduced an alternative method for calculating the instantaneous celerity that is based on the concept of instantaneous frequency from signal processing (Spyrou & Themelis, 2013). The instantaneous frequency is defined as the derivative of the phase of the so-called "analytic signal."

In polar coordinates, an "analytic signal" $Z(t)$ composed of N components can be expressed as:

$$Z(t) = \sum_{i=1}^{N} A_i(t) \cdot \exp\left[j \cdot \varphi_i(t) \right] \tag{4}$$

where $A_i(t)$ and $\varphi_i(t)$ are the instantaneous amplitude and time-dependent phase of the *i*th component, respectively:

$$A_i(t) = \pm\sqrt{z_i^{\,2}(t) + \tilde{z}_i^{\,2}(t)}, \quad \varphi_i(t) = \tan^{-1}\frac{\tilde{z}_i(t)}{z_i(t)} \qquad (5)$$

In (5), $z_i(t)$ and $\tilde{z}_i(t)$ are the real signal and its Hilbert transform, respectively (Feldman, 2011). According to Nho & Loughlin (1999), the instantaneous frequency, in time, for this *N*-component analytic signal will be:

$$\omega(t) = \dot{\varphi}(t) = \left[\sum_i^N A_i^2\,\dot{\varphi}_i + 0.5\sum_{i\neq k}^N A_i\,A_k\,(\dot{\varphi}_i + \dot{\varphi}_k)\cos\Delta\varphi_{ik} + \right.$$
$$\left. + (\dot{A}_i\,A_k - \dot{A}_k\,A_i)\sin\Delta\varphi_{ik}\right] \Big/ \left[\sum_{i=1}^N A_i^2 + \sum_{i\neq k}^N A_i A_k\cos\Delta\varphi_{ik}\right] \qquad (6)$$

where the dot over a function represents the derivative (partial derivative) of that function with respect to time, and $\Delta\varphi_{ik} = \varphi_i - \varphi_k$.

The procedure for calculating the instantaneous celerity at a point entails the localised frequencies in time and in space. We assume that the wave profile is represented, as customarily, by a Fourier series:

$$\zeta(x,\,t) = \sum_{i=1}^N A_i\cos\varphi_i(x,\,t) \qquad (7)$$

The phase of each harmonic component would be $\varphi_i(x,\,t) = k_i x - \omega_i t + \varepsilon_i$, where k_i, ω_i, and ε_i stand for the wave number, the frequency, and the random phase of each harmonic component, respectively. Then, with time marching we specify the locus of points $[x,\,t]$ where the instantaneous celerity will be calculated (an example appears in Fig. 8). At a point $(x_s, t_s) \in [x, t]$, the localized frequencies are calculated by the partial derivatives of phase in time and in space, implying that we freeze, successively, the space and time variable at x_s and t_s in each case:

$$\omega(x_s, t) = -\frac{\partial\varphi(x_s, t)}{\partial t}, \quad k(x, t_s) = \frac{\partial\varphi(x, t_s)}{\partial x} \qquad (8)$$

The partial derivatives are calculated in a manner similar to (6) (the minus sign in the above expression for ω is due to the minus in front of the individual frequencies in the expression for the phase of each harmonic component). The instantaneous celerity at a point in time-space is then directly derived by the following expression:

$$c(x_s, t_s) = \frac{\omega(x_s, t_s)}{k(x_s, t_s)} \qquad (9)$$

Comparisons of wave celerity calculations according to Spyrou, *et al.*, (2012, 2014) and the current scheme are presented below.

Comparison 1: Effect of band-width

A JONSWAP spectrum with significant wave height $H_S = 5$ m and peak period $T_P = 12$ s was used to produce wave realizations with different frequency ranges around the peak (Table 1). Fig. 8 shows contours of the points of zero wave slope—in the *xt*-plane—for the scenario No. 4.

Table 1: Discretization of spectrum and range of frequencies

scenario	% peak (one side)	ω_{start} (rad/s)	ω_{end} (rad/s)	*N* of freq.	Spectrum band-width
1	2.5	0.511	0.537	3	0.014
2	5	0.497	0.550	5	0.029
3	10	0.471	0.576	9	0.057
4	20	0.419	0.628	17	0.108

Fig. 9 compares typical instantaneous celerity curves obtained by the two calculation schemes. The curves follow each other very well, with some small differences noted for the most wide band scenario. The celerity corresponding to the weighted mean frequency is also plotted, it appears to behave like a mean celerity function.

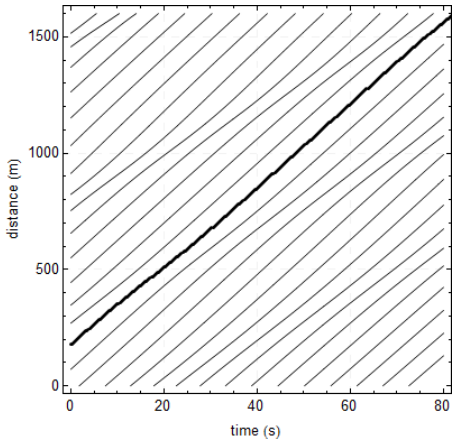

Figure 8: Contours of points of zero slope in wave field (thin lines) and the locus of points where celerity is calculated corresponding to a crest (thick line). The realizations correspond to 4th scenario of Table 1.

Comparison 2: Celerity at ship's position

Ship motion was also involved in the second comparison. Three band-width scenarios were considered (see Table 2), each derived from a JONSWAP spectrum with $H_S = 6$ m and $T_P = 9.5$ s. The ship's nominal speed was 12 m/s. Comparisons of surge velocity against celerity are shown in Fig. 10. The smoother character of the lines obtained by the new celerity calculation scheme is evident, indicating that it would be preferred for the practical implementations of a celerity-based criterion. Surge velocity appears to fluctuate around celerity once surf-riding is established.

Phase Space Topology in Irregular Waves

When addressing the problem of surf-riding in irregular seas, the explicit time dependence of the excitation means that the conventional dynamical

systems toolkit do not provide much help in unraveling the qualitative features of the behavior of the system.

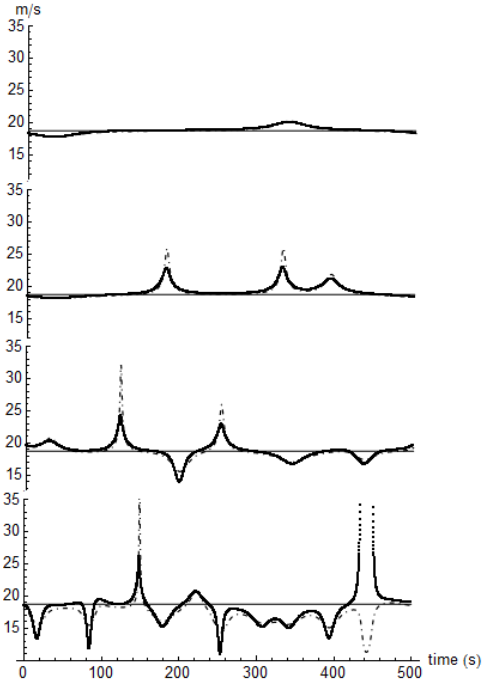

Figure 9: Instantaneous celerity for different wave scenarios (2.5, 5, 10 and 20% of peak period, respectively). Dashed lines correspond to Spyrou, *et al.*, (2012, 2014) while the continuous thick lines are based on the new scheme. The horizontal gray lines stand for the celerity corresponding to the weighted mean wave frequency.

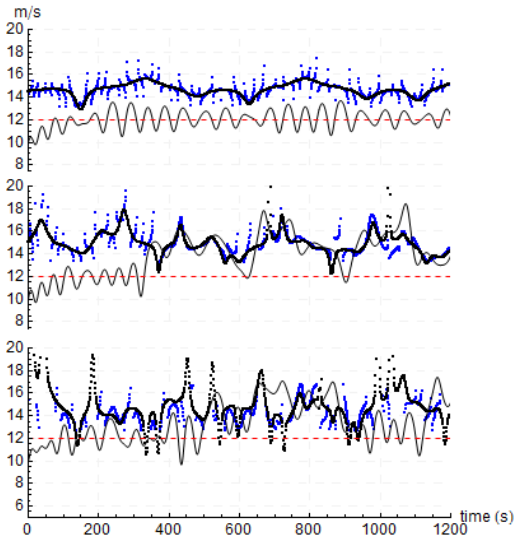

Figure 10: Comparison of instantaneous celerity calculations for different band-widths (5, 10 and 20% of peak period, respectively). Black points refer to the new scheme while the blue to Spyrou, *et al.*, (2012, 2014). The grey curve indicates the ship's surge velocity and the horizontal dashed line is the nominal speed.

It is, however, possible to describe the evolution of the system using a frame of reference that is attached to some key feature of the system itself, where a feature might be any object or structure that is relevant to the problem. In such a case, one has to define the properties of this feature, which is not trivial at all.

Table 2: Data for the "narrow-band" wave realizations

scenario	% peak (one side)	ω_{start} (rad/s)	ω_{end} (rad/s)	N of freq.	Spectrum band-width
1	5	0.628	0.694	4	0.029
2	10	0.595	0.728	7	0.051
3	20	0.529	0.793	13	0.087

The possibility of extracting and tracking features related to the nonlinear surge equation of motion in irregular seas is examined next. The study is based on the concept of Feature Flow Field (Theisel & Seidel, 2003), which addresses the problem of feature tracking in non-stationary flow fields. The Feature Flow Field (FFF) method is proposed for the tracking of a variety of different local features, including critical points of vector fields. Given a vector valued function of the form:

$$v(x,\ y,\ t)=\begin{pmatrix} v_1(x,\ y,\ t) \\ v_2(x,\ y,\ t) \end{pmatrix} \tag{10}$$

a 3-dimensional vector field $V(x, y, t)$ is constructed, by demanding that V points toward the direction of minimal change of v in a first order approximation. This direction is given by the intersection of the planes perpendicular to ∇v_1 and ∇v_2, where the ∇ operator is related to the three-dimensional Euclidian space with coordinates (x, y, t). Thus:

$$V(x,\ y,\ t)=\nabla v_1 \times \nabla v_2 \tag{11}$$

The path of some critical point of v may be seen as a streamline of V, integrated from the point under consideration.

In the case of surf-riding, we usually consider the following system (Spyrou, 2006):

$$\begin{aligned} \dot{x}_1 &= x_2 \\ \dot{x}_2 &= T(x_2)-R(x_2)+F(x_1,\ t) \end{aligned} \tag{12}$$

where x_1 and x_2 are the distance from the origin and the velocity of the ship in the surge direction, respectively, while $T(x_2)$, $R(x_2)$ and $F(x_1, t)$ are the propulsive thrust, ship resistance and surge wave force (all divided by the sum of the mass of the ship and the surge added mass), respectively. It is assumed that (12) is expressed with respect to an earth-fixed coordinate system. The FFF will be given by:

$$V(x_1,\ x_2,\ t)=\nabla \dot{x}_1 \times \nabla \dot{x}_2 \tag{13}$$

An interesting result is observed when we relate the ∇ operator to translating frames of reference, which follow the paths of the phase particles of (12).

Consider for instance (12) with harmonic excitation. The corresponding FFF will be:

$$V\left(x_1,\, x_2,\, t\right)=\begin{pmatrix} V_1\left(x_1,\, x_2,\, t\right) \\ V_2\left(x_1,\, x_2,\, t\right) \\ V_3\left(x_1,\, x_2,\, t\right) \end{pmatrix} \tag{14}$$

We slice the time-extended phase space perpendicular to the *t*-axis and visualize the integral lines of the vector field:

$$V_S\left(x_1,\, x_2;\; t=const\right)=\begin{pmatrix} V_1\left(x_1,\, x_2;\; t=const\right) \\ V_2\left(x_1,\, x_2;\; t=const\right) \end{pmatrix} \tag{15}$$

Then, structures that locally bear strong resemblance to the trajectories around the pair of equilibria (arising as stationary solutions of (12)) can be observed in Fig. 11. In Fig. 11 the integral lines and the magnitude of V_S are shown for the harmonic case. Horizontal lines correspond to wave celerity, while white circles correspond to surf-riding equilibria. These structures occur in connection to certain critical points of (15). It should be noted that the positioning of equilibria agrees with that of the critical points (however, extra critical points of (15) can be found, not relating to equilibrium solutions).

Consider now an analysis of (12) similar to that of the previous paragraph and of Fig. 11, but this time using a JONSWAP wave spectrum (Fig. 12). The "saddle and focus-like" structures are still present. However, these were not observed for all times (when considering the observation window to be of finite size on the phase plane). In Fig. 13 are shown instants of an animated simulation. Streamlines of V_S are visualized in the right part; white circles denote the state of the ship. In many cases the latter appears engaged in a chase with a critical point, appearing as the core of the focus-like structure. Its pair, on the other hand, seems to have a role similar to that of the unstable equilibrium related with surf-riding in harmonic waves: if the ship is "close enough," it accelerates on the downslope of a wave where it engages in a chase of the critical points of (12) mentioned before.

By further consideration of (14) we obtain for the components of *V*:

$$V_1=\frac{dF\left(x_1,\, t\right)}{dt}, \qquad V_2=\dot{x}_2\frac{\partial F\left(x_1,\, t\right)}{\partial x_1} \tag{16}$$

where $dF(x_1, t)/dt$ is the rate of change of $F(x_1, t)$ along the trajectories, *i.e.* the change of the surge wave force as it would be measured by an on-board device. Critical points of (15) appearing as cores of the structures that can be seen in Figs. 11, 12, and 13 are found to satisfy the system of equations:

$$\begin{cases} \dfrac{dF(x_1,t)}{dt}=0 \\ \dot{x}_2=0 \end{cases} \tag{17}$$

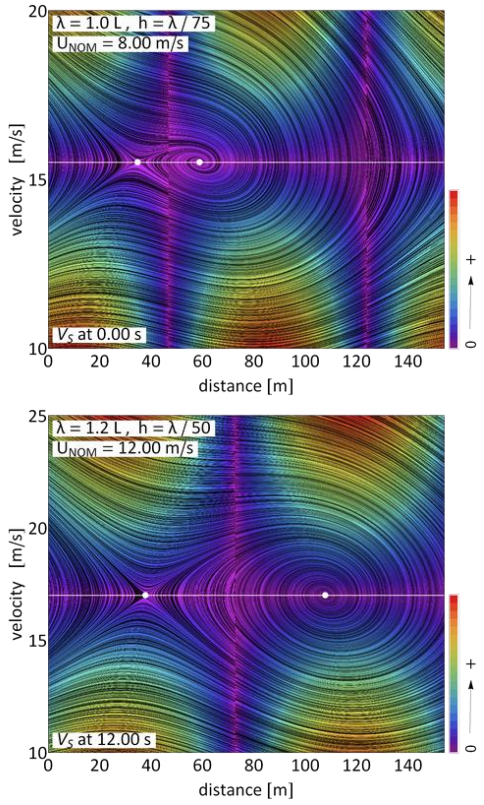

Figure 11: Integral lines and magnitude of V_S for the harmonic case.

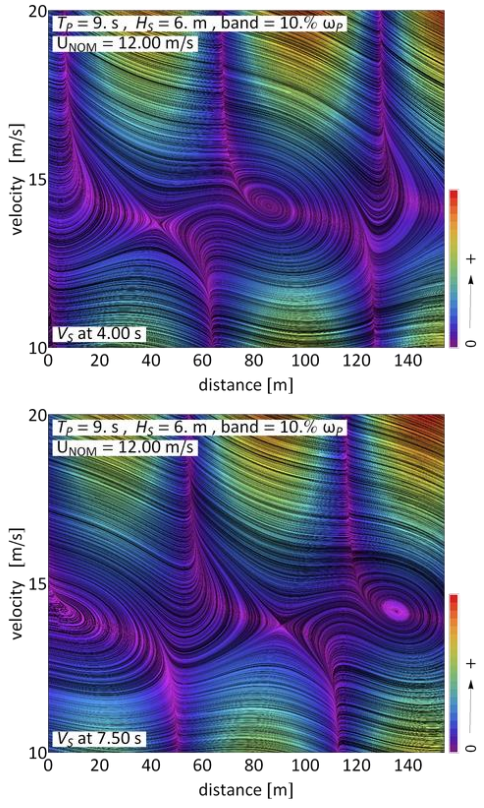

Figure 12: Streamlines and magnitude of V_S for the case of a JONSWAP spectrum.

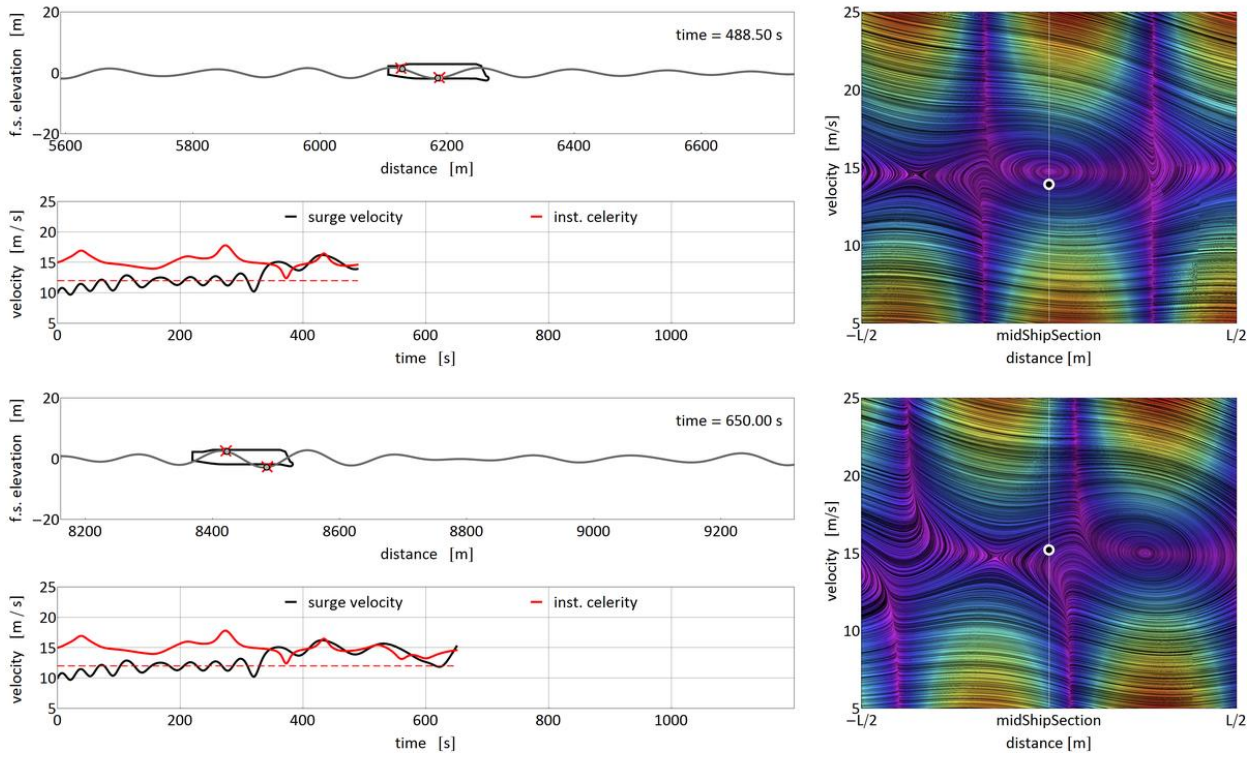

Figure 13: Two instants of an animated simulation for the case of a JONSWAP spectrum ($H_S = 6\ m$, $T_P = 9.5\ s$, frequency range of 20% ω_P and nominal speed set at 12 *m/s*). On the lower left part, one can observe the time history of surge velocity *vs.* that of instantaneous celerity calculated at the ship's position (9). The red dashed line denotes the nominal speed.

which is in fact equivalent to the set of equations:

$$\begin{cases} \ddot{x}_2 = 0 \\ \dot{x}_2 = 0 \end{cases} \tag{18}$$

The latter implies that these are points at which both acceleration and its time derivative attain, instantly, zero values (unfortunately the identified surf-riding states are not the only points satisfying (17) or (18)).

If the velocity $\dot{x}_1$ varies slowly along the path γ of a focus-like critical point, it appears that, the smaller the rate of change, the more γ will be related to a solution. In the extended phase space of (12), γ could be regarded as a core line of a "tube" formed by nearby swirling trajectories. In the harmonic case, this core line is a straight line forming an angle θ with the $x_1 x_2$-plane (and parallel to the $x_1 t$-plane). Furthermore, $\cot\theta = c$ where c denotes the wave celerity.

Possible MPM Metric of Surf-Riding Likelihood

As has been demonstrated in the previous subsection, the introduction of the irregular waves makes the dynamical system time-dependent. Numerical characterization of the invariant manifold, while possible as described above (see also Vishnubholta, *et al.*, 2000), is difficult, has some computational uncertainties, and is time consuming. What would be a good candidate for the metric of surf-riding likelihood? One possibility is the distance to the invariant manifold as shown in Fig. 14.

The invariant manifold is not known and is not expected to be known for the calculation of the metric. However, it is possible to know the position of the

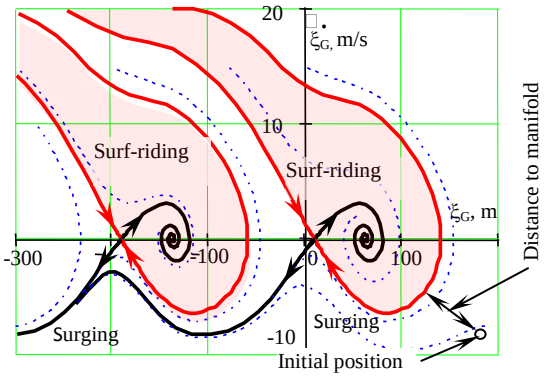

Figure 14: Definition of Possible Candidate for a Metric of Likelihood of Surf-Riding

surf-riding stable quasi-equilibrium. The distance can be measured along the line between the initial position of a ship and position of the stable quasi-equilibrium at the initial instant. The calculation scheme can be similar to the case of pure loss of stability.

To demonstrate that these calculations are viable, consider the surging/surf-riding phase plane with

slowly changing wave characteristics as shown in Fig. 15.

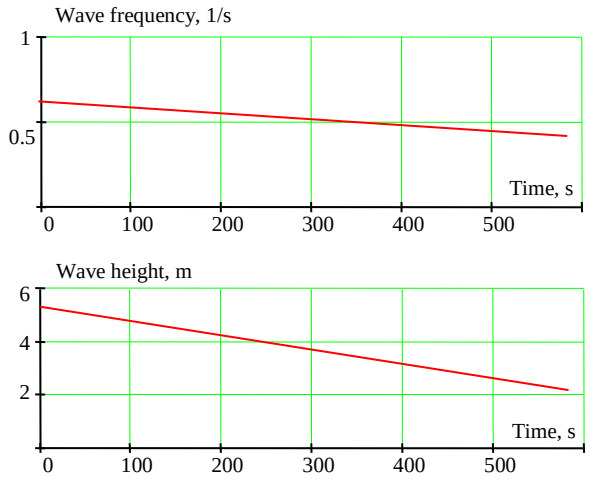

Figure 15: Slowly Changing Parameters of Wave

The changes of the wave parameters shown in Fig. 15 lead to changes in the wave celerity and the positions of the equilibria, as shown in Fig. 16. The equilibria cease to exist around 280 s and surf-riding becomes impossible after that time.

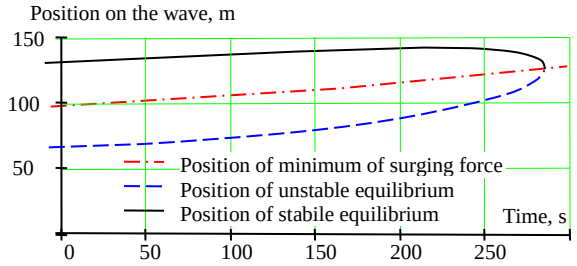

Figure 16: Changes in Positions of the Surf-riding Quasi-Equilibria

The results of iterative perturbations are shown in Fig. 17. One should note that despite its axis of wave position/instantaneous forward speed, the curves shown there are not phase trajectories. The topology of phase plane is changing; it would be more correct to think of Fig 17 as a projection of 3D curves, where the third dimension is time. Nevertheless, the perturbations do work the same way as the case of pure loss of stability. The critical point, indeed, belongs to the invariant manifold at the initial instant of time.

CONCLUSIONS AND FUTURE WORK

Several dynamical aspects related to the application of the split-time method to pure loss of stability and to surf-riding have been presented.

Some pure loss of stability occurrences may be related to duration and phasing of stability deterioration. A critical roll rate at the instant of upcrossing at an intermediate level was defined as the minimum roll rate that would lead to capsizing and can be evaluated through an iterative application of perturbations called the Motion Perturbation Method (MPM). Through the MPM method, it was demonstrated that ship stability in waves is a particular case of motion stability of a dynamical system.

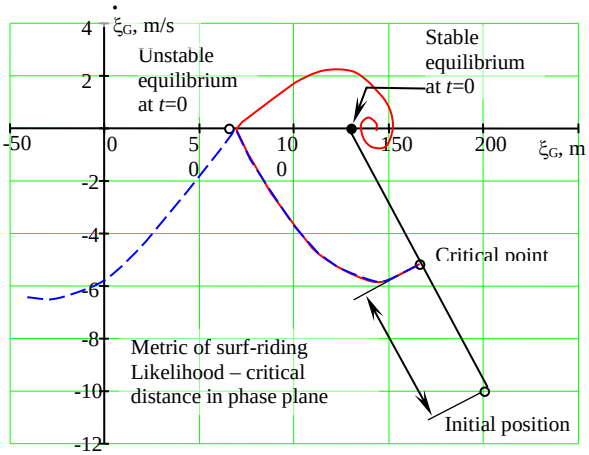

Figure 17: Calculation of Critical Distance in Phase Plane

The difference between the instantaneous and critical roll rate can be used as a MPM metric for the likelihood of capsizing due to pure loss of stability as it includes the changes of stability in waves without any assumptions. The choice of the intermediate level is mostly a computational issue, as only independent MPM metrics can be used for further calculations.

A key issue for surf-riding in irregular waves is the definition of wave celerity. The positions of quasi-equilibria depend on celerity, so the celerity affects the phase-plane arrangement. A new method for calculating wave celerity is proposed, based on the concept of instantaneous frequency. It provides a smoother celerity curve in comparison with the definition based on the speed of propagation of characteristic features (such as the maximum wave slope angle).

The irregularity of the waves renders the phase plane time-dependent. Conventional analysis based on stationary phase flows cannot help in this case. Methods from fluid mechanics applied to time-dependent real flows can also help for phase flows. We have introduced the “Feature Flow Field” method for tracking different local features of the phase flow, which play an organizing role for the phase flow in their vicinity.

The straight-line distance, in the phase plane, between the state of a ship and the position of stable surf-riding quasi-equilibrium at that instant may be considered as a candidate MPM metric of the likelihood of surf-riding in irregular waves.

ACKNOWLEDGEMENTS

The work described in this paper has been funded by Drs. Patrick Purtell and Ki-Han Kim at U.S. Office of Naval Research (ONR) and Dr. Woei-Min Lin at ONR Global. Furthermore, our discussions with Prof. Pol Spanos (Rice University) have been very fruitful.

REFERENCES

Beck, R. F. & A. M. Reed (2001) "Modern Computational Methods for Ships in a Seaway." Trans. SNAME, 109, pp 1–48.

Belenky, V., J. Spyrou, K. M. Weems & W.-M. Lin (2013) "Split-time Method for the Probabilistic Characterization of Stability Failures in Quartering Waves." Int'l. Shipbuilding Progress, 60(1–4):579–612.

Belenky, V., K. Weems, B. Campbell, T. Smith & V. Pipiras (2014) "Extrapolation and Validation Aspects of the Split-Time Method." Proc. 30th Symp. on Naval Hydrodynamics, Hobart, Tasmania, Australia.

Belenky, V., K. M. Weems & W.-M. Lin (2008) "Numerical Procedure for Evaluation of Capsizing Probability with Split Time Method." 27th Symp. on Naval Hydrodynamics, Seoul, Korea.

Belenky, V. L., K. M. Weems, W.-M. Lin & K. J. Spyrou (2010) "Numerical Evaluation of Capsizing Probability in Quartering Seas with Split Time Method." Proc. 28th Symp. on Naval Hydrodynamics, Pasadena, CA, USA.

Bishop, R. C., W. Belknap, C. Turner, B. Simon & J. H. Kim (2005) "Parametric Investigation on the Influence of GM, Roll Damping, and Above-Water Form on the Roll Response of Model 5613." Carderock Division, Naval Surface Warfare Center Report NSWCCD-50-TR-2005/027.

Dunwoody, A. B. (1989a) "Roll of a Ship in Astern Seas—Metacentric Height Spectra." J. Ship Research, 33(3):221-228.

Dunwoody, A. B. (1989b) "Roll of a Ship in Astern Seas—Response to GM Fluctuations." J. Ship Research, 33(4):284–290.

Euler, L. (1749) Scientea Navalis, St. Petersburg, Russia.

Feldman, M. (2011) Hilbert Transform Applications in Mechanical Vibration, West Sussex, UK: John Wiley & Sons, Ltd.

Lin, W.-M. & D. K. P. Yue (1990) "Numerical Solutions for Large Amplitude Ship Motions in the Time-Domain." Proc. 18th Symp. on Naval Hydrodynamics., Ann Arbor, MI, pp. 41–66.

Nho, W. & P. J. Loughlin (1999) "When is Instantaneous Frequency the Average Frequency at Each Time?" IEEE Signal Processing Letters, 6(4):8–80.

Paulling, J. R. (1961) "The Transverse Stability of a Ship in a Longitudinal Seaway." J. Ship Research, 4(4):37–49.

Paulling, J. R., O. H. Oakley & P. D. Wood (1975) "Ship Capsizing in Heavy Seas: The Correlation of Theory and Experiments." Proc. 1st Int'l. Conf. on Stability of Ships and Ocean Vehicles, Glasgow.

Pollard, J. & A. Dudebout (1892) Theorie du Navire, Tome III. Dynamique du Navire: Mouvement de Roulis sur Houle, Mouvement Rectiligne Horizontal Direct (Résistance des Carènes) Paris: Gauthier-Villars et Fils.

Spyrou, K. J. (1996) "Dynamic Instability in Quartering Seas: The Behavior of a Ship During Broaching." J. Ship Research, 40(1):46–59.

Spyrou, K. J. (2006) "Asymmetric Surging of Ships in Following Seas and its Repercussions for Safety." Nonlinear Dynamics, 43:149–172.

Spyrou, K. J., V. Belenky, N. Themelis & K. Weems (2012) "Conditions of Surf-Riding in an Irregular Seaway." Proc. 11th Int'l. Conference on Stability of Ships and Ocean Vehicles, STAB 2012, Athens, Greece.

Spyrou, K. J., V. Belenky, N. Themelis & K. Weems (2014) "Detection of Surf-riding Behavior of Ships in Irregular Seas." Nonlinear Dynamics, DOI 10.1007/s11071-014-1466-2.

Spyrou, K. & N. Themelis (2013) "Wave Celerity in a Multi-Chromatic Sea: A Comparative Study." Proc. 13th Int'l. Ship Stability Workshop, Brest, France.

Spyrou, K. & I. Tigkas (2011) "Nonlinear Surge Dynamics of a Ship in Astern Seas: "Continuation Analysis" of Periodic States with Hydrodynamic Memory." J. Ship Research, 55(1):19-28.

Spyrou, K. J., K. M. Weems & V. Belenky (2009) "Verification of the Patterns of Surf-riding and Broaching by an Advanced Hydrodynamic Code." Proc. 10th Int'l. Conference on Stability of Ships and Ocean Vehicles, St. Petersburg, Russia.

Theisel, H. & H.-P. Seidel (2003) "Feature Flow Fields." Data Visualization 2003. Proc. VisSym 03, pp. 141–148.

Vishnubholta, S., J. Falzarano & A. Vakakis (2000) "A New Method to Predict Vessel/Platform Critical Dynamics in a Realistic Seaway." Phil. Trans. of the Royal Soc. of London: Series A—Mathematical Phys. and Eng. Sciences, 358:1967–1981.